Clim. Past Discuss., 2, 923–949, 2006
www.clim-past-discuss.net/2/923/2006/

Climate of the Past Discussions

Climate of the Past Discussions is the access reviewed discussion forum of *Climate of the Past*

The modern and glacial overturning circulation in the Atlantic ocean in PMIP coupled model simulations

S. L. Weber[1], S. S. Drijfhout[1], A. Abe-Ouchi[2], M. Crucifix[3], M. Eby[4], A. Ganopolski[5], S. Murakami[6], B. Otto-Bliesner[7], and W. R. Peltier[8]

[1]Royal Netherlands Meteorological Institute (KNMI), De Bilt, The Netherlands
[2]Center for Climate System Research, The University of Tokyo Kashiwa, Japan
[3]Hadley Center for Climate Prediction and Research, Met Office, Exeter, United Kingdom
[4]School of Earth and Ocean Sciences, University of Victoria, Victoria, Canada
[5]Potsdam Institute for Climate Impact Research, Potsdam, Germany
[6]Meteorological Research Institute, Tsukuba, and Frontier Research Center for Global Change, JAMSTEC, Yokohama, Japan
[7]National Center for Atmospheric Research, Boulder, U.S.A.
[8]Department of Physics, University of Toronto, Toronto, Canada

Received: 22 September 2006 – Accepted: 5 October 2006 – Published: 11 October 2006

Correspondence to: S. L. Weber (weber@knmi.nl)

Abstract

The simulation of the Atlantic thermohaline circulation (THC) during the Last Glacial Maximum (LGM) provides an important benchmark for models used to predict future climatic changes. This study analyses the THC response to LGM forcings and boundary conditions in nine PMIP simulations, including both GCMs and Earth system Models of Intermediate Complexity. It is examined whether the mechanism put forward in the literature for a glacial THC reduction in one model also plays a dominant role in other models. In five models the THC reduces during the LGM (by 5–40%), whereas four models show an increase (by 10–40%). In all models but one a reduced (enhanced) THC goes with a stronger (weaker) reversed deep overturning cell associated with the formation of Antarctic Bottom Water (AABW). It is found that a major controlling factor for the THC response is the density contrast between AABW and North Atlantic Deep Water (NADW) during the LGM as compared to the modern climate. More saline AABW is consistently found in all simulations, while all models but one show less cooling of AABW as compared to NADW. In five out of nine models a reduced (enhanced) THC during the LGM is associated with more (less) dense AABW at its source region, which in turn is determined by the balance between the opposing effects of salinity and temperature on the density of AABW versus that of NADW. The response in net evaporation over the Atlantic basin is relatively small in most models, so that changes in the freshwater budget are dominated by ocean transports. In only two models is the THC response during the LGM directly related to the response in net evaporation.

1 Introduction

Simulation of the glacial climate provides an important test for general circulation models (GCMs) used to predict future climate changes. The Paleoclimate Modeling Intercomparison Project (PMIP) has defined a standard set of forcings and boundary conditions for the Last Glacial Maximum (LGM) and pre-industrial climate in order to facilitate

CPD

2, 923–949, 2006

intercomparison among models and with paleoclimatic data (e.g. Masson-Delmotte et al., 2005; Kageyama et al., 2006). During the first phase of PMIP, simulations were done with atmospheric GCMs. Now that simulations of the glacial climate with coupled atmosphere-ocean GCMs are feasible, it is possible to test the glacial Atlantic thermohaline circulation (THC) against the available evidence from proxy data. Paleoclimatic data suggest that the overturning cell associated with North Atlantic Deep Water (NADW) formation was weaker than today (McManus et al., 2004), with enhanced intrusion of Antarctic Bottom Water (AABW) into the Atlantic basin (Duplessy et al., 1988; Curry and Oppo, 2005). Models, on the other hand, show a wide range of responses when comparing the glacial THC to the modern. The Atlantic THC is intensified in some of the first coupled AO-GCM runs (Hewitt et al., 2001; Kitoh et al., 2001), while it is weakened in others (Peltier and Solheim, 2003; Shin et al, 2003). Considering this diversity of GCM results, the mechanism underlying the reconstructed glacial THC changes remains to be established.

Several hypotheses have been put forward in the literature on the dominant forcing for the reduced glacial THC in the Atlantic ocean. Sensitivity experiments with the UVic intermediate-complexity coupled model show that the glacial thermal forcing alone leads to stronger NADW formation, while diminished net evaporation over the Atlantic basin counteracts the thermal forcing resulting in reduced NADW (Schmittner et al., 2002). The glacial ocean exhibits two closely related equilibrium states in the CLIMBER-2 intermediate-complexity model, which differ in the location of deep-water formation (Ganopolski et al., 1998; Ganopolski and Rahmstorf, 2001). One is a stable "cold" mode with a slightly weakened THC, due to a salinity reduction in NADW compared to AABW, and the other a marginally unstable "warm" mode with a more northern formation of NADW and intensified THC. Finally, a weakened THC in the Atlantic ocean is associated with enhanced AABW formation induced by stronger equatorward sea-ice export in the Southern Ocean in the NCAR AO-GCM (Shin et al., 2003).

In this paper we compare the modern and glacial circulation in the Atlantic ocean simulated by coupled atmosphere-ocean models within the framework of PMIP. More

specifically, we examine whether the mechanism put forward in the literature for a glacial THC reduction in one model also plays a dominant role in other models. The focus is on the Atlantic freshwater budget and the competition between NADW and AABW.

2 Models and experimental design

The present intercomparison study includes five PMIP2 coupled AO simulations (Table 1), that have been integrated long enough to have allowed the deep ocean to adjust to glacial boundary conditions. Two of the GCMs (CCSM and HadCM) start from the cold state of a previous coupled LGM simulation, whereas one GCM (MIROC) is initialized from modern conditions. We include two Earth system Models of Intermediate Complexity (EMICs; ECBilt/CLIO and the UVic model), which both consist of a simplified atmospheric component while the ocean/sea-ice component is similar in complexity to those in the AO-GCMs. The two EMIC runs start from a warm state, but have each been run for a few millennia under glacial forcings and boundary conditions.

The PMIP2 forcings for the LGM, which occurred ca. 21000 years Before Present (21 kyr BP), are the changes in solar insolation and the reduced concentrations of Greenhouse Gases relative to the pre-industrial control state. Boundary conditions are the ICE-5G ice-sheet reconstruction (Peltier, 2004) and the changes in land-sea mask consistent with ICE-5G. The lowering of sea level due to the presence of large continental ice sheets results in exposed land, most notably in the circum-Atlantic area is the closure of Bering Strait. Vegetation and other land-surface characteristics are unchanged with respect to the control simulation. The forcings and boundary conditions are detailed on the PMIP2 website (www-lsce.cea.fr/pmip2/).

For some of the coupled AO models included in the present analysis earlier LGM simulations have been published, using the ICE-4G ice-sheet reconstruction (Peltier, 1994) in which the Fennoscandian ice sheet extended far east over northwestern Siberia. These so-called PMIP1.5 runs exist for HadCM (Hewitt et al., 2001), UVic (Schmittner

et al., 2002), the NCAR CCSM (Shin et al., 2003) and the University of Toronto version of the CCSM model (CCSM1.4; Peltier and Solheim, 2003). In the present study, the most recent PMIP2 simulations are used for CCSM (Otto-Bliesner et al., 2006) and UVic. For HadCM we analyse both the PMIP2 and the earlier PMIP1.5 runs, as they exhibit a qualitatively different THC response. In addition, we analyse the early MRI (Kitoh et al., 2001) and CCSM1.4 runs (Peltier and Solheim, 2003) as well as the "cold" glacial state found in CLIMBER-2 (Ganopolski et al., 1998). The latter model is an EMIC consisting of a zonally-averaged three-basin ocean component coupled to a statistical-dynamical atmosphere.

Some variations exist among the PMIP simulations in the handling of ice-sheet melt and the adaptation of the river routing scheme. In all control simulations the maximum snow depth is set to a fixed limit (of 1–2 m). When it exceeds this limit, excess snow melts and becomes runoff. Most models retain this method for the LGM simulations, whereas Hadl2 includes a predetermined freshwater flux to the high–latitude oceans (200 mm/year in the Arctic and in the Atlantic, poleward of 50° N, and 80 mm/year poleward of 50° S). These fluxes were calibrated such as to compensate for the long-term accumulation of snow over the adjacent ice sheets. For the Atlantic/Arctic basin this is equivalent to a freshwater forcing of 0.13 Sv during the LGM. The present-day river pathways are used for the LGM in most models. Only Hadl2 and ECBilt adopt a slight modification. In the Hadl2 run the river pathways were altered according to the output from a river routing model forced with ICE-5G topography. In ECBilt/CLIO those catchment areas that are covered by ice-sheets during the LGM are added to the catchment of a nearby non-covered river. Mean ocean salinity includes an increase of 1 PSU in the LGM initial state of CCSM (Shin et al., 2003), but is left unchanged in all other PMIP runs.

3 The Atlantic thermohaline circulation

Data indicate a slowdown of the Atlantic THC during the LGM as compared to the present climate by ca. 30%, and probably less (McManus et al., 2004). Most likely the location of deep-water formation was more southward than today. Formation of NADW resulted in a shallower overturning, with the southward moving North Atlantic water mass centered at ca. 1500 m depth (Curry and Oppo, 2005). Deep water of southern origin penetrated as far north as 60° N into the Atlantic basin, with its effect evident as shallow as 2000 m (Curry and Oppo, 2005). At present NADW is warm and saline, whereas AABW is cold and relatively fresh. During the LGM the Southern Ocean contained the saltiest deep water (Adkins et al., 2002).

In five model simulations (CCSM, Hadl2, UVic, UTor and ClimC) the Atlantic overturning circulation indeed slows down, see Table 2. In those runs the maximum overturning strength Ψ_{max} is reduced by 1–6 Sv (3–40%) during the LGM as compared to the control state. In four simulations (MIROC, ECBilt, Hadl1.5 and MRI) the THC strength increases by 2–7 Sv (9–40%). In all simulations, except UVic, the location of the THC maximum shifts southward or remains at the same latitude. There is no relation between the amplitude of the southward shift and the response in THC strength. The THC mostly shoals (deepens) in those simulations that show a decrease (increase) in THC strength. The UVic model shows a deepening of the center of the Atlantic circulation cell, but a shoaling of the division between the THC and the reversed deep cell. There is a shouthward shift of the location of NADW formation sites. We thus find reasonable agreeement with the data in the response of the strength and the depth of the overturning cell for five models.

The strength Ψ_S of the reversed cell associated with the intrusion of AABW increases (decreases) for decreasing (increasing) strength of the Atlantic overturning in all models, except Hadl1.5. In case of a stronger Ψ_S during the LGM AABW penetrates deeper into the Atlantic basin and at shallower depths. Here we find reasonable agreement with the data for six models, but the reversed cell remains at depths below 3000 m and

latitudes south of 40–50° N in most of these models.

4 The Atlantic freshwater budget

As a first step in the analysis this section examines the response of net evaporation over the Atlantic basin, which has been hypothesized to strongly affect the response in THC strength (Schmittner et al., 2002). The water loss due to net evaporation should be balanced by oceanic transports into the basin (Rahmstorf, 1996). We consider all terms in the freshwater budget rather than just the surface freshwater forcing, as any change in one term will affect the other terms of the budget in order to achieve equilibrium.

4.1 The terms of the freshwater budget

The Atlantic freshwater budget consists of a surface flux component (net evaporation) and several oceanic components (transport through the boundaries). Mass conservation imposes that in equilibrium all components should balance:

$$[E_{net}] = M_{ov} + M_{az} + M_{dif} + M_{BS}. \quad (1)$$

Here the surface flux contribution $[E_{net}]$ is the net basin-integrated result of evaporation, precipitation, continental run-off, ice-melt and brine rejection. It also includes any water flux correction, if this is applied in a particular model. The meridional overturning component M_{ov} and azonal component M_{az} of the oceanic freshwater transport through the southern boundary are defined as (Rahmstorf, 1996):

$$M_{ov} = -\frac{1}{S_0}\int dz\, \overline{v}(z)[< S(z) > -S_0], \quad (2)$$

$$M_{az} = -\frac{1}{S_0}\int dz\, \overline{v'(z)S'(z)}, \quad (3)$$

where S_0 is a reference salinity, the overbar and the brackets $< \ . \ >$ denote zonal integration and zonal averaging, respectively, and v' and S' are deviations from zonal means. The other terms of Eq. (1) represent contributions from diffusion at the southern boundary and transport through Bering Strait. The southern border of the Atlantic basin ranges from 31.5 to 34.5° S in the different ocean GCMs. It is taken to be at 40° S in the CLIMBER-2 zonal-mean ocean component, as the closure coefficient between the meridional and zonal pressure gradient is reduced by three orders of magnitude at this latitude.

In the present analysis we compute M_{ov} and M_{az} from the mean seasonal cycle (monthly values) of the 3-D fields of northward velocity v and ocean salinity S that are available in the PMIP database. The run length that is used to compute the mean seasonal cycle ranges from 10–100 yr. Comparison for ECBilt with results based on 100-year timeseries of daily output indicates that this is fairly accurate. The total freshwater flux $[E_{net}]$ is also available from the database, but for most models not its separate components. The Bering Strait and diffusive contributions are determined as rest term $R=[E_{net}]- M_{ov}-M_{az}$ from Eq. (1), assuming that the freshwater budget has equilibrated. In practice, R also contains a term that is associated with the drift in basin-mean salinity in the Atlantic basin. A number of models incorporate the freshwater flow through Bering Strait for the pre-industrial climate, either parameterised as a diffusive transport or explicitly calculated. This transport is mostly set to zero in the LGM simulations, see Table 1.

The overturning component can be understood as the net freshwater transport carried by the THC. For negative values of M_{ov} the THC *exports* freshwater, even though the Atlantic is a net evaporative basin. The "excess" salt is removed by the azonal component M_{az}, which incorporates the export of surface and thermocline waters via the subtropical gyre. The direction of the overturning freshwater transport is hypothesized to be closely related to the dynamical regime of the THC (Rahmstorf, 1996): for a (partly) thermal driven THC a southward transport (M_{ov} negative) implies that a stable circulation state without NADW formation is also possible. It is not trivial whether

such a conceptual model can be applied to GCMs or the real world. However, M_{ov} was shown to be a good diagnostic for the stability of the THC in ECBilt simulations by Vries and Weber (2005).

4.2 The pre-industrial and glacial freshwater budgets

For the present-day climate [E_{net}] is thought to carry a net freshwater transport of 0.2–0.3 Sv out of the Atlantic basin (Pardaens et al., 2003). Using inverse-model data Weijer et al. (1999) have suggested that the present-day ocean has M_{az} = 0.38 Sv and M_{ov} = −0.20 Sv. These estimates are compared to PMIP simulations in Fig. 1. Net evaporation is positive in all models, except MRI where it is just below zero. This term is overestimated by 0.1–0.3 Sv in most simulations. All models, except ECBilt, have positive M_{ov} which is most likely at variance with observations. Most models understimate the azonal term M_{az}. (It is zero by definition in ClimC, because this model only resolves the zonal-mean Atlantic circulation.)

The rest term is small enough in most models to assume that diffusion and remaining imbalances play a secondary role. However, for some models the freshwater budget has not yet fully equilibrated. This implies that the budget terms might change when continuing these runs over longer integration times and only preliminary conclusions can be drawn from the present results. Freshwater is not conserved in the UTor model, giving rise to a weak secular variation in mean ocean salinity (Peltier and Solheim, 2003).

The differences (LGM minus pre-industrial values) show a reduction of net evaporation in the cold LGM climate in all PMIP simulations, except Hadl1.5 and MRI. The changes are most pronounced in Hadl2 and UTor, where [E_{net}] is reduced by 0.1–0.2 Sv, and in MRI, where [E_{net}] increases by 0.2 Sv. In all other models, there are larger changes in the ocean transport terms than in the surface flux term. This implies that the response of the freshwater budget at 21 kyr BP is more determined by oceanic processes than by, for example, changes in precipitation, river run-off or sea-ice formation. The ocean overturning transport increases (considerably) in most models,

whereas the azonal component is mostly reduced during the LGM. Those models that close Bering Strait during the LGM mostly show a reduction in the amplitude of the rest term.

4.3 The surface freshwater forcing as a function of latitude

There is local net evaporation in the subtropics, while there is local net precipitation in the equatorial region and in the mid-high latitudes in all pre-industrial control simulations, broadly consistent with observations. The meridionally-integrated values are shown in Fig. 2 as a function of latitude. In the northern part of the Atlantic basin the integrated values are negative (net precipitation) up to ca. 20° N in all models, except MRI. However, the basin-integrated value is positive (net evaporation), because of the subtropical evaporation zones which dominate over the net precipitation at mid-high latitudes and in the equatorial region. The EMICs underestimate the amplitude of latitudinal variations, but capture the basic pattern. In the UTor run [E_{net}] is overestimated considerably, because the tropical precipitation belt is almost completely absent in this model. The latitudinal variations of net evaporation generated by the atmospheric part of the MRI model are basically similar to the other models, but the local flux adjustment is quite large especially over the northern Atlantic. The latitudinal profile of the surface freshwater forcing given to the OGCM is, therefore, more complex in the MRI model.

Latitudinal response patterns (Fig. 2) show a southward shift of the northern Atlantic net precipitation in six models (CCSM, Hadl2, MIROC, MRI, UTor and ClimC), with decreased high-latitude net precipitation and increased mid-latitude net precipitation during the LGM as compared to the control run. However, in most models the net effect is small. Only in the UTor simulation there is a clear increase of the mid-high latitude net precipitation during the LGM. Of the three other models ECBilt and UVic show an increased net precipitation over the northern Atlantic, while there is little change in the Hadl1.5 simulation. Over the equatorial and southern Atlantic ocean all models seem to show a latitudinal pattern of reduced subtropical evaporation as well as reduced tropical precipitation, with amplitudes varying among the different models. The

basin-integrated value [E_{net}] is thus the result of a subtle balance between different processes. It shows little change during the LGM (less than 0.05 Sv) in all simulations except Hadl2, MRI and UTor. The latitudinal distribution in Hadl2 indicates that reduced subtropical evaporation in the colder LGM climate plays a major role in reducing [E_{net}] in this model, while both reduced subtropical evaporation and increased mid-high latitude precipitation are important for UTor. In the MRI simulation tropical precipitation reduces considerably during the LGM, so that [E_{net}] increases.

4.4 The ocean transport through the southern boundary

All models, except UTor, simulate very saline surface and thermocline waters at the southern border of the Atlantic ocean, below which relatively fresh Antarctic intermediate waters lie (Fig. 3). The upper "limb" of the THC consists of these waters flowing northward while undergoing transformations due to, for example, the surface freshwater forcing. The lower "limb", NADW flowing southward, lies roughly between 1000 m and 3000 m depth. In most models it is more saline than the upper limb for the modern climate, as indicated by the positive value of M_{ov} (the THC imports freshwater). Antarctic bottom water is slightly fresher than NADW in all simulations, except the two HadCM runs, UTor and ClimC. In these simulations NADW and AABW have similar salinity (Hadl1.5 and ClimC) or AABW is even more saline than NADW (Hadl2, UTor).

During the LGM most models simulate somewhat fresher surface and thermocline waters and more saline water at deeper levels. The response is most pronounced in CCSM, which simulates an increase of 0.5–1.7 PSU in Atlantic water masses below ca. 1000 m (not taking the global-mean increase by 1 PSU in this model into account). Most models simulate a stronger increase in salinity in AABW than in NADW. In the ClimC simulation AABW becomes more saline, while NADW even freshens. In some models (MIROC, UVic, UTor) changes in deep-ocean salinity are minor. The MRI model shows a freshening at all levels.

Most models simulate a larger M_{ov} during the LGM, because the fresh upper limb of the THC freshens and the saline lower limb becomes more saline. This effect is

so strong, that a larger M_{ov} is even found in those models which simulate a decrease in the overturning strength. It can be amplified by a strong intensification of the THC as, for example, in the MIROC run. Only in case of a pronounced decrease in Ψ_{max} there is a decrease in the overturning transport term (UVic, UTor). In the MRI run M_{ov} decreases, because the lower THC branch freshens.

Significant contributions to M_{az} come from depths above ca. 700 m. This is in accordance with the longitudinal variations of salinity being appreciable only at those depths. All models exhibit a salinity maximum near the South American continent, resulting in a positive M_{az} for the control climate. The azonal component becomes smaller during the LGM compared to modern in most models. This is mainly due to a reduced zonal contrast in the southern Atlantic ocean salinity, while the gyre circulation intensifies. In two models (UVic and UTor) the azonal salinity contrast becomes stronger, resulting in an enhanced azonal transport.

4.5 Preliminary conclusions

Changes in the overturning freshwater transport are clearly not a good diagnostic for changes in THC strength, as ΔM_{ov} is mostly positive or close to zero irrespective of $\Delta\Psi_{max}$. Also, we cannot attribute the change in THC strength to one of the other components of the freshwater budget. It seems that none of these terms can be seen as the main driver for the changes in Atlantic overturning. So we reject the earlier hypothesis that changes in Atlantic net evaporation primarily cause changes in Atlantic overturning, when comparing modern and LGM values. Clearly, the Atlantic overturning does not operate in isolation and is not forced locally by the Atlantic freshwater budget. The most likely candidate from outside to drive changes in the Atlantic overturning seems to be the Southern Ocean overturning cell involving AABW formation. There is a remarkable anticorrelation between the response in this cell and that in the overturning strength (compare Table 2). In the next section we will evaluate the interaction between the Southern Ocean and Atlantic overturning cells in more detail.

The response of the overturning transport term does give an indication of the sta-

bility of the THC during the LGM as compared to present. Most models exhibit increased stability during the LGM in the sense that larger freshwater perturbations are needed to cause a permanent collapse of the circulation. In terms of the hysteresis diagram: the system is on the thermohaline (monostable) branch and further away from the bifurcation to the thermal regime where a stable mode with collapsed THC exists. Monostability of the glacial THC was already demonstrated by Ganopolski and Rahmstorf (2001) in the CLIMBER-2 model, where a collapsed LGM state does not exist (but which allows for two closely-related modes with an active THC during the LGM). Also, the glacial THC was found to be monostable in experiments with an ocean-only model by Prange et al. (2002). The present results suggest that most models exhibit similar behavior, as the positive value of M_{ov} indicates that they are on the thermohaline branch during the LGM. For two models (ECBilt and UVic) the LGM state is very close to the bifurcation point between the thermohaline and thermal branches ($M_{ov} \simeq 0$), which might cause a strongly nonlinear response to the imposed LGM forcings and boundary conditions.

5 Southern Ocean controls versus Atlantic processes

In this section we examine the THC response during the LGM, focussing on the role of processes within the Atlantic basin versus those originating in the Southern Ocean. To characterise the controlling processes within the Atlantic basin, we examine both the response in net evaporation $\Delta[E_{net}]$ and the response in the density difference $\Delta\rho_{Atl}$ between the northern and southern ends of the Atlantic basin. The density difference, which is ultimately generated by local fluxes of heat and freshwater at the ocean surface, has been found to scale linearly with the overturning strength in a number of modelling studies (Hughes and Weaver, 1994; Rahmstorf, 1996; Thorpe et al., 2001). If the THC response is controlled by Atlantic processes, then one expects $\Delta\Psi_{max}$ to scale with $\Delta[E_{net}]$ and $\Delta\rho_{Atl}$. On the other hand, if the competition between NADW and AABW plays a major role (Ganopolski et al., 1998; Shin et al., 2003) such scaling

behavior is less likely.

In the following the Atlantic north-south density difference ρ_{Atl} is computed as the difference between the zonal- and depth mean density in the northern Atlantic (at 55° N) and at the southern end of the Atlantic basin (taken at 30° S in all models). The former is assumed to characterise the density of NADW at its source region, as the location of the sinking branch of the meridional overturning cell associated with NADW is at ca. 55° N in most models. The depth average is taken over depths between the surface and 1500 m. The latter depth level lies within the body of southward flowing NADW for most models at the two time periods. This choice of level of integration was found to be adequate for the HadCM3 model (Thorpe et al., 2001), while no sensitive dependence of the scaling relation on the depth level was found by Rahmstorf (1996).

Changes in the overturning strength are plotted against changes in net evaporation in Fig. 4 (upper left diagram). For most models there is a clear relationship between the sign of $\Delta\Psi_{\max}$ and $\Delta[E_{net}]$. However, the amplitude of changes in THC strength does not seem to depend much on the amplitude of changes in $[E_{net}]$. These results indicate that small changes in the freshwater forcing (of 0.05 Sv and less) during the LGM as compared to modern are not decisive for the simulated THC response. However, a strong reduction or increase in $[E_{net}]$ (as in Hadl2, MRI and UTor) clearly contributes toward a THC reduction or increase.

Changes in the overturning strength scale with $\Delta\rho_{Atl}$ in only three out of nine models (Fig. 4, upper right diagram): an increased ρ_{Atl} gives rise to a stronger overturning in MIROC and Hadl1.5, while a decreased ρ_{Atl} and reduced $\Psi_{\max}$ are found in UTor. In the six other models, the response in the density difference works against the response in overturning strength. Examination of the north-south temperature and salinity differences (Fig. 4, lower diagrams) does not show a consistent response among the different models. The northern part of the Atlantic basin cools more than the southern part in some models, and vice versa in others. Also, the northern Atlantic freshens in some models and becomes more saline in others compared to the southern part.

Next we consider changes in the density of AABW at its source latitude and associ-

ated changes in the reversed circulation cell at depths below ca. 3000 m in the Atlantic ocean. The strength of the reversed cell increases (decreases) consistently with reduced (increased) Ψ_{max} for the LGM climate as compared to the control climate in all simulations except Hadl1.5 (Fig. 5, upper left diagram). This suggests that changes in AABW density play an important role in controlling changes in the Atlantic THC strength. The density of AABW is characterised here by the zonal-mean density at 55°S averaged over all depth levels. The density contrast ρ_{SN} is defined as the density difference between AABW (at 55°S) and NADW (at 55°N). The density contrast varies greatly among the different models in the control state. High ρ_{SN} is found in those models that have relatively saline AABW at the southern end of the Atlantic basin (Hadl2 and UTor; compare Fig. 3), while in one model (ECBilt) ρ_{SN} is slightly negative.

Changes in Ψ_{max} are shown versus those in ρ_{SN} in Fig. 5 (upper right diagram). The response in the density contrast is a fairly good predictor for the response in Atlantic overturning strength in most models that have a significant change in ρ_{SN}. A relative increase in AABW density is found in CCSM, UTor and ClimC, together with an increased Ψ_S and decreased Ψ_{max}. The reverse is seen in MIROC and Hadl1.5, while three models (Hadl2, ECBilt and MRI) have very small $\Delta\rho_{SN}$. In one model (UVic) the density contrast reduces, while Ψ_{max} reduces as well. The response in temperature and salinity contrast (Fig. 5, lower diagrams) is more consistent than in case of the Atlantic north-south differences. During the LGM AABW becomes relatively more saline in all models, while it cools less than NADW in all models except one. The opposing effects of temperature and salinity on the density contrast result in an increased density contrast in some models, but decreased contrast others.

6 Discussion and conclusions

This paper analyses the response of the Atlantic overturning circulation to LGM forcings and boundary conditions in nine PMIP coupled model simulations. Central in the analysis is the question of which mechanism ultimately controls the THC response: changes

in net evaporation over the Atlantic basin, local processes within the Atlantic basin as expressed by the density difference between the northern and southern ends, or the deep overturning cell associated with the formation of AABW in the Southern Ocean. The results are summarised in Table 3. It is found that in two simulations (CCSM and ClimC) the controlling process originates exclusively in the Southern Ocean: AABW is more dense during the LGM as compared to the control climate, the reversed deep cell in the Atlantic ocean intensifies and AABW penetrates more northward and at shallower depth into the basin, resulting in a shallower and weaker THC. The response in the Atlantic density contrast ρ_{Atl} opposes the THC response in these two models, while net evaporation remains close to modern values during the LGM.

In three other simulations (MIROC, Hadl1.5 and Utor) both the response in the density contrast ρ_{SN} between AABW and NADW and in the Atlantic density contrast ρ_{Atl} play a role. Here $\Delta\rho_{SN}$ and $\Delta\rho_{Atl}$ have the same sign, so that it is not possible to distinguish between the two factors. In one of these simulations (Utor) changes in $[E_{net}]$ contribute toward the simulated THC response, whereas it is small in the other two runs. In two simulations (Hadl2 and MRI) the response in $[E_{net}]$ seems to be the controlling process. Finally, for two simlations (ECBilt and Uvic) it is not possible to identify which process dominates the simulated THC response.

We thus find that $\Delta\rho_{SN}$ is a major controlling factor. It is determined by the balance between an increase in AABW salinity versus a relative warming (less cooling) as compared to NADW during the LGM. More saline AABW during the LGM is consistently found in all simulations, but the amplitude of the signal varies considerably. A strong increase as suggested by Adkins et al. (2002) is only found in CCSM. In this model the salinity increase is attributed to sea-ice expansion rather than changes in evaporation and precipitation (Shin et al., 2003). Further research is needed to establish whether this mechanism is unique to the CCSM model or whether it is also present in other models, but less active than in CCSM.

It is remarkable that net evaporation over the Atlantic basin only plays a dominant role in two simulations. In one of these (Hadl2) the reduction in $[E_{net}]$ during the LGM

is partly due to an imposed freshwater flux at high northern latitudes. In the earlier HadCM run (Hadl1.5), which did not contain such a freshwater forcing, the THC response is dominated by density contrasts rather than $\Delta[E_{net}]$. Although evaporation decreases in the colder LGM climate, precipitation and run-off also decrease resulting in a small net effect in most simulations. Interestingly, most models that have a THC reduction during the LGM show a decrease in net precipitation over the northern Atlantic ocean. This implies that it is definitely not a high-latitude freshening of the Atlantic basin which causes the glacial THC reduction.

It is not possible to pinpoint the controlling mechanism in two simulations (ECBilt and UVic). Changes in the controlling factors discussed above are too small to attribute the relatively large THC changes found in these two models to any of them. In the case of ECBilt the very low density of AABW in the control climate may play a role. Obviously, this favours a THC increase when LGM forcings and boundary conditions are imposed. In the UVic model the THC strength decreases during the LGM, which is inconsistent with the simulated $\Delta\rho_{SN}$. Both models have an overturning freshwater transport close to zero during the LGM, indicating that these models are close to the bifurcation point where the collapsed THC exists (Rahmstorf, 1996; Vries and Weber, 2005). This may give rise to a strongly nonlinear response, in agreement with the large THC changes associated with the small changes in the controlling factors found in these models.

Acknowledgements. The Laboratoire des Sciences du Climat et de l'Environnement (LSCE) is acknowledged for collecting and archiving the model output. The PMIP2 Data Archive (www-lsce.cea.fr/pmip2/) is supported by CEA, CNRS, the EU project MOTIF (EVK2-CT-2002-00153) and the Programme National d'Etude de la Dynamique du Climat (PNEDC). The analyses were performed using output available at 29-08-2006. This research was partly funded by the MOTIF project. M. Kliphuis is thanked for developing the post-processing software.

References

Adkins, J. F., McIntyre, K., Schrag, D. P.: The salinity, temperature and $\delta^{18}O$ of the glacial deep ocean, Science, 298, 1769–1773, 2002.

Curry, W. B., and Oppo, D. W.: Glacial water mass geometry and the distribution of $\delta^{13}C$ of ΣCO_2 in the western Atlantic ocean, Paleoceanography, 20, 1017–1028, 2005.

Duplessy, J. C., Shackleton, N. J., Fairbanks, R. G., Labeyrie, L., Oppo, D. W., and Kallel, N.: Deep water source variations during the last climatic cycle and their impact on the global deep water circulation, Paleoceanography, 3, 343–360, 1988.

Ganopolski, A. and Rahmstorf, S.: Rapid changes of glacial climate simulated in a coupled model, Nature, 409, 153–158, 2001.

Ganopolski, A., Rahmstorf, S., Petoukhov, V., and Claussen, M.: Simulation of modern and glacial climates wih a coupled global model of intermediate complexity, Nature, 391, 351–356, 1998.

Hewitt, C. D., Broccoli, A. J., Mitchell, J. F., and Stouffer, R. J.: A coupled model study of the last glacial maximum: was part of the North Atlantic relatively warm?, Geophys. Res. Lett., 28, 1571–1574, 2001.

Kageyama, M., Laine, A., Abe-Ouchi, A., Braconnot, P., Cortijo, E., M. Crucifix, M., de Vernal, A., Guiot, J., Hewitt, C.D., Kitoh, A., Marti, O., Ohgaito, R., Otto-Bliesner, B., Peltier, W. R., Rosell-Mele, A., Vettoretti, G., Weber, S. L., and MARGO Project Members: Last Glacial Maximum temperatures over the North Atlantic, Europe and western Siberia: a comparison between PMIP models, MARGO sea-surface temperatures and pollen-based reconstructions, Quatern. Sci. Rev., 25(17–18), 2082–2102, 2006.

Kitoh, A., Murakami, S., and Koide, H.: A simulation of the Last Glacial Maximum with a coupled atmosphere-ocean GCM, Geophys. Res. Lett., 28, 2221–2224, 2001.

Masson-Delmotte, V., Kageyama, M., Braconnot, P., Charbit, S., Krinner, G., Ritz, C., Guilyardi, E., Jouzel, J., Abe-Ouchi, A., Crucifix, M., Gladstone, R. M., Hewitt, C. D., Kitoh, A., Legrande, A. N., Marti, O., Merkel, U., Motoi, T., Ohgaito, R., Otto-Bliesner, B., Peltier, W.R., Ross, I., Valdes, P. J., Vettoretti, G., Weber, S. L., Wolk, F., and Yu, Y.: Past and future polar amplification of climate change: climate model intercomparison and ice-core constraints, Climate Dyn., 26(5), 513–529, doi:10.1007/s00382-005-0081-9, 2005.

McManus, J., Francois, R., Gherardi, J., Keigwin, L., and Brown-Leger, S.: Collapse and rapid resumption of Atlantic meridional circulation linked to deglacial climate changes, Nature, 428,

834–837, 2004.
Otto-Bliesner, B., Brady, E. C., Clauzet, G., Tomas, R., Levis, S., and Kothalava, Z.: Last Glacial Maximum and Holocene climate in CCSM3, J. Climate, 19, 2526–2544, 2006.
Pardaens, A. K., Banks, H. T., Gregory, J. M., and Rowntree, P. R.: Freshwater transports in HadCM3, Climate Dyn., 21, 177–195, 2003.
Peltier, W. R.: Ice age paleotopography, Science, 265, 195–201, 1994.
Peltier, W. R.: Global glacial isostasy and the surface of the ice-age Earth: the ICE-5G (VM2) model and GRACE, Ann. Rev. of Earth and Plan. Sciences, 32, 111–149, 2004.
Peltier, W. R., and Solheim, L. P.: The climate of the Earth at Last Glacial Maximum: statistical equilibrium state and a mode of internal variability, Quat. Sci. Rev., 23, 335–357, 2004.
Prange, M., Romanova, V., and Lohmann, G.: The glacial thermohaline circulation: stable of unstable?, Geophys. Res. Lett., 29, 2028–2031, 2002.
Rahmstorf, S.: On the freshwater forcing and transport of the Atlantic thermohaline circulation, Climate Dyn., 12, 799–811, 1996.
Shin, S., Liu, Z., Otto-Bliesner, B., Kutzbach, J. E., and Vavrus, S. J.: Southern ocean sea-ice control of the glacial North Atlantic thermohaline circulation, Geophys. Res. Lett., 30, 1096, doi:10.1029/2002GL015513, 2003.
Schmittner, A., Meissner, K. J., Eby, M., and Weaver, A. J.: Forcing of the deep ocean circulation in simulations of the Last Glacial Maximum, Paleoceanography, 17, 2002.
Thorpe, R. B., Gregory, J. M., Johns, T. C., Wood, R. A., and Mitchell, J. F. B.: Mechanisms determining the Atlantic Thermohaline circulation response to Greenhouse Gas forcing in a non-flux-adjusted coupled climate model, J. Climate, 14, 3102–3116, 2001.
Vries, P. de and Weber, S. L.: The Atlantic freshwater budget as a diagnostic for the existence of a stable shut-down of the meridional overturning circulation, Geophys. Res. Lett., 32, L09606, doi:10.1029/2004GL021450, 2005.
Weijer, W., de Ruijter, W. P. M., Dijkstra, H. A., and van Leeuwen, P. J.: Impact of interbasin exchange on the Atlantic overturning circulation, J. Phys. Oceanogr., 29, 2266–2284, 1999.

Table 1. The simulations that are included in the analysis, abbreviated model names, type of atmospheric component, the number of ocean horizontal grid points (lonxlat) and depth levels, the number of years at the end of each simulation used to compute the overturning streamfunction in section 3 and the mean seasonal cycle in section 4, and the time periods for which the model allows for transport through Bering Strait. The ocean component of CLIMBER-2 contains three zonally-averaged basins.

model (country)	abbreviation	type of atmosphere	ocean grid	output segment	Bering Strait
PMIP2 simulations					
CCSM3.0 (USA)	CCSM	GCM	320x395x40	10	0k
HadCM3M2 (UK)	Hadl2	GCM	288x144x20	100	0k
MIROC3.2 (Japan)	MIROC	GCM	256x192x43	50	0k, 21k
ECBilt/CLIO (Netherlands)	ECBilt	quasi-geostr. GCM	120x60x20	100	0k
UVic (Canada)	UVic	moist EBM	100x100x19	10	-
PMIP1.5-type simulations					
HadCM3 (UK)	Hadl1.5	GCM	288x144x20	50	0k
MRI-CGCM1 (Japan)	MRI	GCM	144x111x23	40	0k, 21k
CCSM1.4 (Canada)	UTor	GCM	100x116x25	100	-
CLIMBER-2 (Germany)	ClimC	stat.dyn. model	3*x72x20	100	-

Table 2. The THC maximum Ψ_{max} (in Sv; occurring at the given latitude and depth) for 0 kyr and 21 kyr BP and same for the maximum Ψ_S at the southern boundary of the Atlantic basin of the reversed cell associated with AABW. The last column gives the response in the THC maximum $\Delta\Psi_{max}$ (in Sv and as a percentage of the modern value).

	$\Psi_{max,\ 0k}$	$\Psi_{max,\ 21k}$	$\Psi_{S,\ 0k}$	$\Psi_{S,\ 21k}$	$\Delta\Psi_{max}$
PMIP2					
CCSM	20.8 (40° N, 1379)	17.3 (28° N, 918)	–3.7	–6.6	–3.5 (17%)
Hadl2	17.4 (34° N, 996)	16.9 (34° N, 996)	–5.7	–5.9	–0.5 (3%)
MIROC	18.8 (35° N, 1125)	26.1 (35° N, 1300)	–4.3	–2.4	+7.3 (39%)
ECBilt	13.8 (35° N, 850)	18.4 (26° N, 1718)	–3.4	0.0	+4.7 (25%)
UVic	20.4 (37° N, 1006)	14.2 (42° N, 1251)	–3.0	–3.6	–6.2 (30%)
PMIP1.5-type					
Hadl1.5	18.3 (34° N, 996)	21.7 (33° N, 996)	–6.2	–6.5	+3.4 (19%)
MRI	27.1 (44° N, 950)	29.5 (36° N, 1300)	–4.7	–2.3	+2.4 (9%)
UTor	21.6 (35° N, 819)	13.1 (30° N, 662)	–3.1	–6.6	–5.1 (40%)
ClimC	23.0 (50° N, 1000)	18.4 (50° N, 500)	–2.9	–5.7	–4.6 (20%)

CPD
2, 923–949, 2006

EGU

Table 3. Overview of the scaling relationships between the response in THC strength and in net evaporation [E_{net}], the Atlantic density contrast ρ_{Atl} and the contrast ρ_{SN} between AABW and NADW, with Yes (?yes) indicating a strong (weak) relationship, No (?no) indicating a clear (likely) absence of any relation and a blank indicating no significant response in the controlling process. The fifth column summarizes the controlling processes for each model. The last two columns show in which control simulations AABW is extremely dense or light compared to NADW and which LGM simulations have an overturning freshwater transport close to zero.

	$[E_{\text{net}}]$	ρ_{Atl}	ρ_{SN}	control	AABW_{0k}	$M_{\text{ov, 21k}}$
PMIP2						
CCSM	?yes	No	Yes	ρ_{SN}		
Hadl2	Yes	No		$[E_{\text{net}}]$	dense	
MIROC	?no	Yes	Yes	$\rho_{\text{Atl}}+\rho_{\text{SN}}$		
ECBilt		No			light	$\simeq 0$
UVic		?no	No			$\simeq 0$
PMIP1.5-type						
Hadl1.5	?yes	Yes	Yes	$\rho_{Atl}+\rho_{\text{SN}}$		
MRI	Yes			$[E_{\text{net}}]$		
UTor	Yes	Yes	Yes	$[E_{\text{net}}]+\rho_{\text{Atl}}+\rho_{\text{SN}}$	dense	
ClimC		No	Yes	ρ_{SN}		

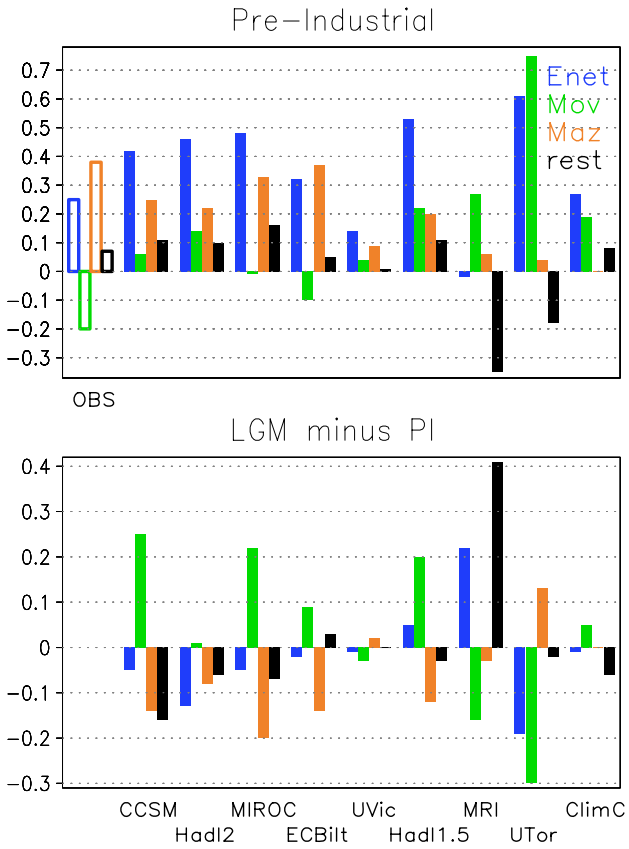

Fig. 1. The terms of the Atlantic freshwater budget as defined in Eq. (1) for the pre-industrial control state (upper panel) and the difference between the LGM and the control state (lower panel) for the PMIP simulations as indicated on the horizontal axis. The terms (in Sv) are net evaporation (blue), the overturning (green), azonal (orange) and rest term (black). Open bars denote "observed" values, see text.

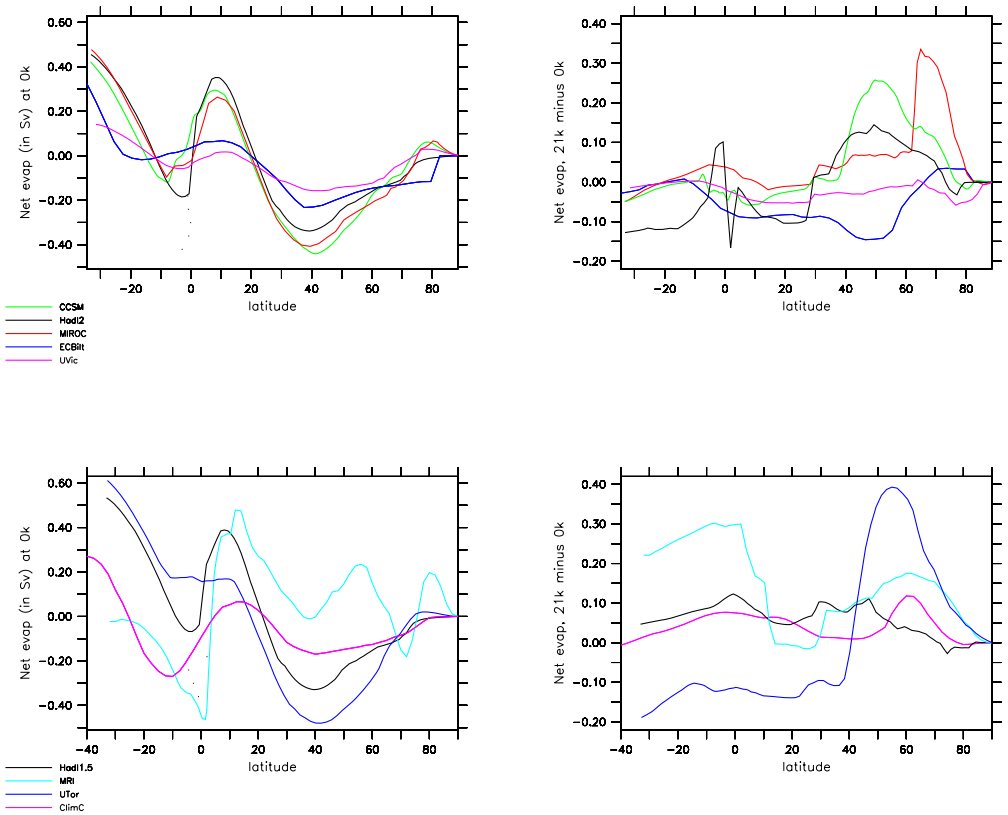

Fig. 2. Meridionally-integrated net evaporation over the Atlantic basin as a function of latitude for the pre-industrial control state (upper left panel) and the difference between the LGM and the control state (upper right panel) for the PMIP2 simulations: CCSM (green), Hadl2 (black), MIROC (red), ECBilt (dark blue) and UVic (purple). Same for the PMIP1.5-type simulations (lower panels): Hadl1.5 (black), MRI (light blue), UTor (dark blue) and ClimC (purple). The integration starts at 90° N (compare Fig. 1 for the values at the southern border).

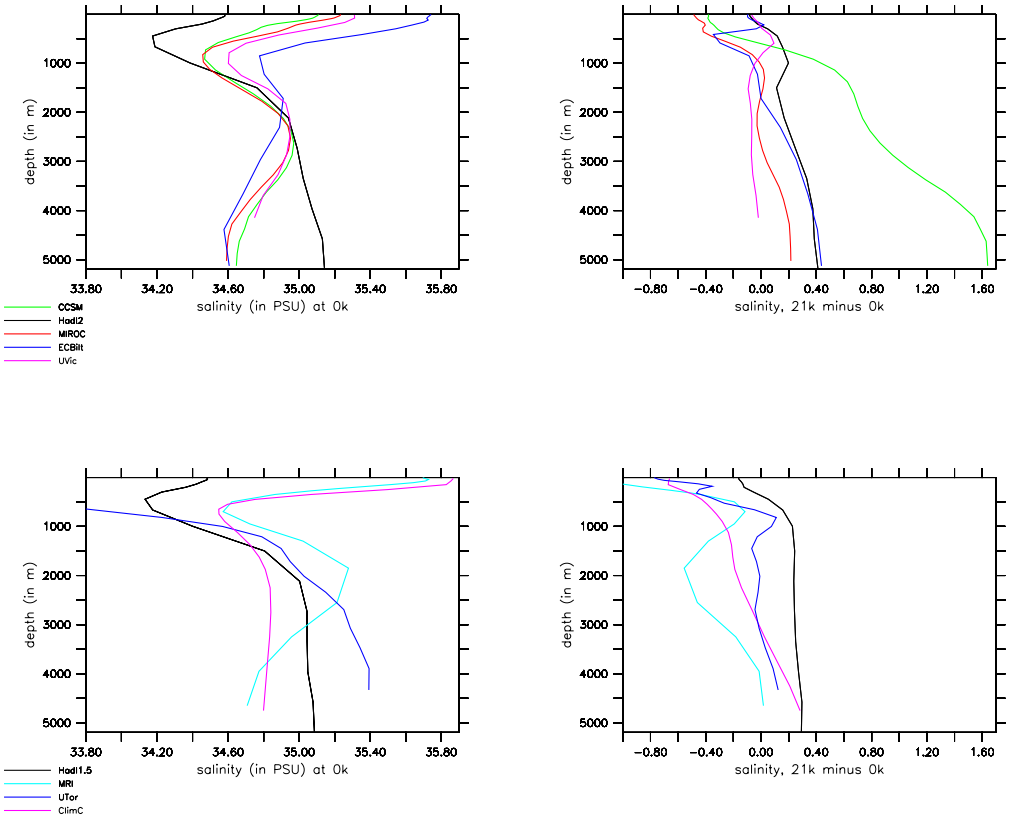

Fig. 3. The zonal-mean salinity at the southern border of the Atlantic basin as a function of depth for the control state (upper left panel) and the difference between the LGM and the control state (upper right panel) for the PMIP2 simulations. Same for the PMIP1.5-type simulations (lower panels). Color coding as in Fig. 2. The global-mean 1 PSU increase for the LGM in the CCSM model has been subtracted from the model output in order to facilitate comparison with the other models.

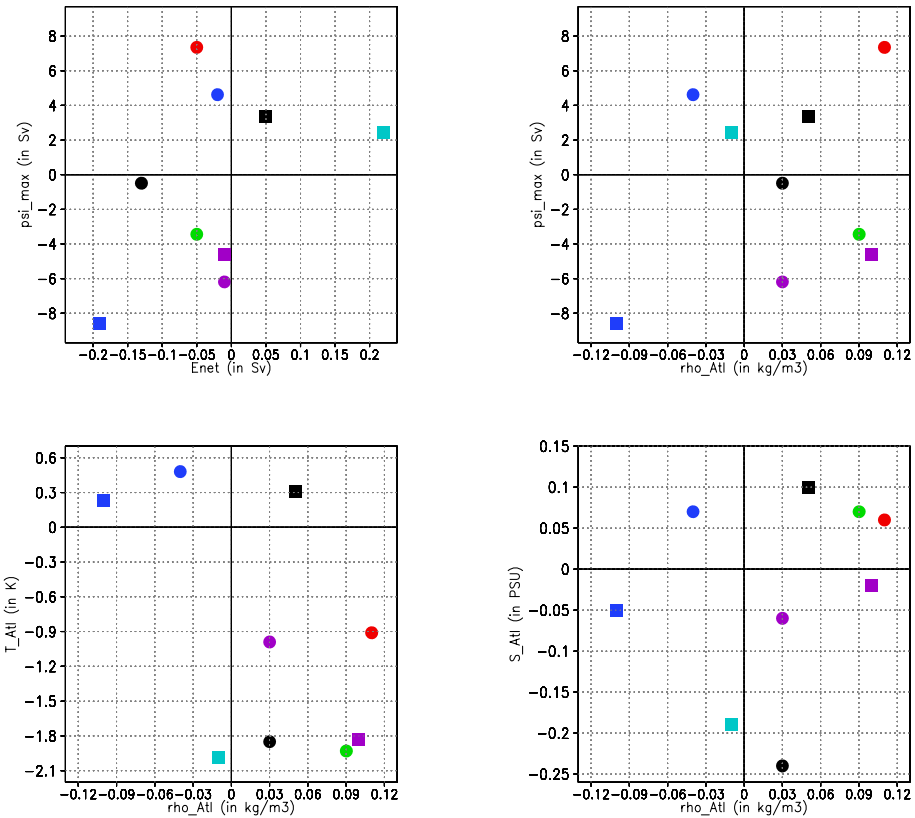

Fig. 4. The response in the maximum of the Atlantic THC strength versus that in net evaporation (upper left panel) and versus that in the north-south Atlantic density difference ρ_{Atl} (upper right panel) for the PMIP2 (circles) and PMIP1.5 (squares) simulations. Color coding as in Fig. 2. The lower panels give the response in the north-south Atlantic temperature difference and salinity difference versus $\Delta\rho_{Atl}$: negative values on the vertical axis indicate that the northern Atlantic cools and freshens during the LGM as compared to the southern part.

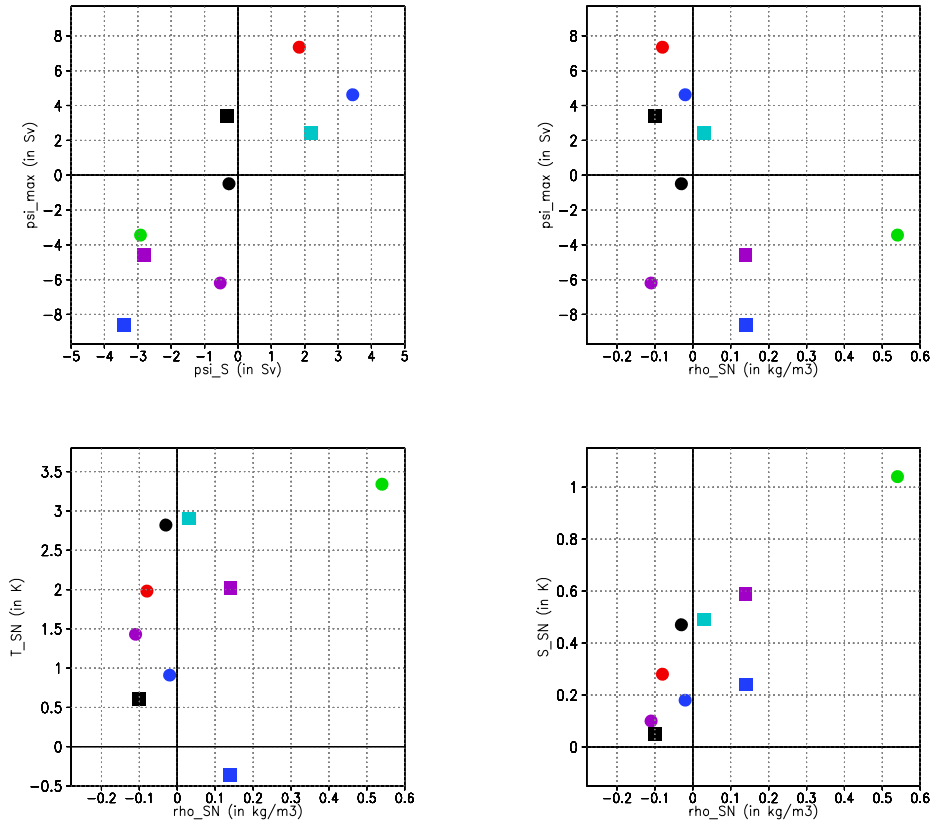

Fig. 5. The response in the maximum of the Atlantic THC strength versus that in the maximum of the deep reversed cell associated with AABW (upper left panel) and versus that in the density contrast ρ_{SN} between AABW and NADW (upper right panel). Symbols and colors as in Fig. 4. The lower panels give the response in the contrast in temperature and salinity between AABW and NADW versus $\Delta\rho_{SN}$: positive values on the vertical axis indicate that AABW cools less and becomes more saline during the LGM as compared to NADW.